

A Super-Twisting sliding mode control combined with a fuzzy logic scheme for improving electric power steering performance

Tuan Anh Nguyen^{1*}, Duc Ngoc Nguyen¹, Thang Binh Hoang², and Thi Hien Duong¹

Abstract: This paper presents the design of a robust control mechanism that integrates the Super-Twisting Sliding Mode Control with a fuzzy logic scheme (FSTSMC). The selected control law mitigates chattering effects while maintaining a simple structural form. The theoretical stability of the closed-loop system is examined using Lyapunov criteria to guarantee convergence. The control parameter is adjusted through a fuzzy mechanism with two inputs to improve the system's adaptability to parameter uncertainties, which are typically neglected in conventional control law design. Numerical simulation results demonstrate that the proposed controller achieves superior tracking performance compared with conventional SMC. Specifically, the Root Mean Square (RMS) tracking error does not exceed 0.04% in the absence of parameter uncertainties and remains below 3.55% when uncertainties are considered, except for the motor current (5.867%). In addition, the proposed scheme significantly suppresses chattering, which is still seen in conventional SMC.

Keywords: Electric power steering, super-twisting sliding mode control, parameter uncertainties, vehicle dynamics.

1. Introduction

Most cars today have assisted-power steering systems to reduce steering effort and make steering easier. EPS systems provide many advantages over traditional power steering systems. Baharom et al. have asserted that EPS is more energy-saving and environmentally friendly than hydraulic power steering (Baharom et al., 2013). Li et al. have stated that EPS has a simple structure and high reliability, and is easy to install on most popular car models (Li et al., 2019). In addition, EPS systems also provide a better driving feel and can maintain stability and safety when steering at high speeds.

Several studies on the control of EPS systems have been published recently. Hassan et al. designed a Proportional–Integral–Derivative (PID) controller for a small-sized vehicle equipped with EPS (Hassan et al., 2012). The control parameters were tuned using a Genetic Algorithm (GA) within a simple framework, although the stability of the controller was not addressed. A more flexible approach was later presented in (Zheng and Wei, 2023), where the PID parameters were adaptively adjusted through a fuzzy logic system. Their results showed that yaw rate overshoot was reduced by 72.9%, while tracking accuracy improved by 75.2%. In (Lee et al., 2019), the authors developed a lead–lag controller combined with a disturbance observer to enhance EPS performance.

Zhao and Zhang conducted a comparative study of PID and H_∞ controllers, revealing that the steering wheel torque under PID control exhibited considerable overshoot. In contrast, H_∞ control substantially mitigated the issue (Zhao and Zhang, 2018). Applications of Linear Quadratic Gaussian (LQG) and Linear Quadratic Tracking (LQT) controllers for EPS have also been explored (Irmer and Henrichfreise, 2020; Nguyen, 2025). However, two of these methods require full state availability, which can degrade system performance when the measured signals are affected by sensor noise. More recently, a discrete time Sliding Mode Control (SMC) scheme for improving EPS performance was introduced (Kim et al., 2023).

Most of the above publications have ignored the influence of parameter uncertainties, which can significantly affect control performance. This study proposes a robust control algorithm for EPS, developed within the framework of Sliding Mode Control to address this drawback. The effect of parameter uncertainties is explicitly considered by incorporating an upper bound of the lumped disturbance into the control law.

The remainder of the paper is organized into four sections. The first section provides an overview and a review of the related literature. The following section describes the system dynamics and the controller design. Simulation results are presented and discussed in the third section. Finally, the conclusion section concludes the paper with key remarks and observations.

2. Mathematical models

The structure of an EPS system is illustrated in Figure 1a, which consists of a steering column, a steering wheel, a rack and pinion, a DC motor, a motor gear, and sensors.

¹Automotive Engineering Division, Thuyloi University

²School of Mechanical Engineering, Hanoi University of Science and Technology

* Corresponding author

Received 24th Nov. 2025

Accepted 23rd Dec. 2025

Publication date 31st Dec. 2025

The system dynamics are presented in equations (1), (2), and (3), where θ_c is steering column angle, θ_m is steering motor angle, i_m is motor current, u is control input, T_d is driver torque, K_c is steering column stiffness, B_c is steering column damping, J_c is steering column inertia, N is motor gear ratio, r_p is pinion radius, K_t is torque coefficient, L_m is motor inductance, and R_m is motor resistance. Equivalent damping (B_{eq}) and equivalent inertia (J_{eq}) are determined according to (4) and (5), where B_m is the steering motor damping, B_r is the rack damping, J_m is the steering motor inertia, and m_r is the rack mass. Road reaction torque (T_r) is approximately calculated according to (6), where l_c is caster trail, l_n is arm length, γ_k is kingpin angle, and γ_c is caster angle.

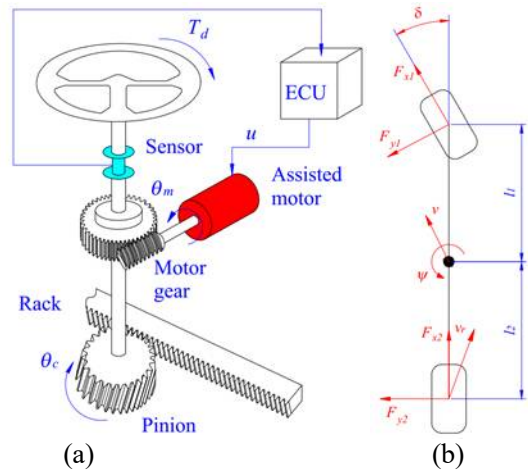


Figure 1. Dynamic models.
(a) EPS model (b) Vehicle model

$$J_c \ddot{\theta}_c + B_c \dot{\theta}_c + K_c \left(\theta_c - \frac{\theta_m}{N} \right) = T_d \quad (1)$$

$$J_{eq} \ddot{\theta}_m + B_{eq} \dot{\theta}_m + \frac{K_c + K_r r_p^2}{N^2} \theta_m = \frac{K_c}{N} \theta_c + K_t i_m - \frac{T_r}{N} \quad (2)$$

$$K_t \dot{\theta}_m + L_m \dot{i}_m + R_m i_m = u \quad (3)$$

$$B_{eq} = B_m + B_r \frac{r_p^2}{N^2} \quad (4)$$

$$J_{eq} = J_m + m_r \frac{r_p^2}{N^2} \quad (5)$$

$$T_r \approx r_p l_c F_{y1} \frac{\cos^2 \gamma_k \cos^2 \gamma_c}{l_n} \quad (6)$$

A linear single-track dynamic model is utilized to determine variation in tire force (Figure 1b). Equations (7), (8), and (9) are established based on the D'Alembert principle, where m is vehicle mass, v_x is longitudinal velocity, v_y is lateral velocity, ψ is yaw angle, J_ψ is yaw inertia, δ is steering angle, F_x is longitudinal force, F_y is lateral force, l_i are distance

from center to axles. In the linear dynamic model, the longitudinal force is assumed to be approximately zero during low-speed steering maneuvers. In contrast, the lateral force depends on the cornering stiffness (K_α) and the lateral sideslip angle (α), as expressed in equation (10). Set the state variables in the order in (11).

$$m(\dot{v}_x - v_y \dot{\psi}) = F_{x1} \cos \delta + F_{x2} - F_{y1} \sin \delta \quad (7) \quad J_\psi \ddot{\psi} = l_1 (F_{x1} \sin \delta + F_{y1} \cos \delta) - l_2 F_{y2} \quad (9)$$

$$m(\dot{v}_y + v_x \dot{\psi}) = F_{y1} \cos \delta + F_{y2} + F_{x1} \sin \delta \quad (8) \quad F_y \approx K_\alpha \alpha \quad (10)$$

$$[x_i] = [\theta_c \quad \dot{\theta}_c \quad \theta_m \quad \dot{\theta}_m \quad i_m] \quad (11)$$

By differentiating the state variables, equations (12) to (16) are obtained. The control error (e) is defined as in (17), where x_{ref} is the reference signal. The sliding surface (s) is formulated as given in (18). The super-

twisting control law (u_{st}) is proposed as in (19) and (20), where k_1 and k_2 are positive coefficients. By taking the derivative of the sliding surface and combining it with (16), equation (21) is obtained.

$$\dot{x}_1 = x_2 \quad (12) \quad \dot{x}_2 = -\frac{K_c}{J_c} x_1 - \frac{B_c}{J_c} x_2 + \frac{K_c}{J_c N} x_3 + \frac{T_d}{J_c} \quad (13)$$

$$\dot{x}_3 = x_4 \quad (14) \quad \dot{x}_4 = \frac{K_c}{J_{eq} N} x_1 - \frac{K_c + K_r r_p^2}{J_{eq} N^2} x_3 - \frac{B_{eq}}{J_{eq}} x_4 + \frac{K_t}{J_{eq}} x_5 - \frac{T_r}{J_{eq} N} \quad (15)$$

$$\dot{x}_5 = -\frac{K_t}{L_m} x_4 - \frac{R_m}{L_m} x_5 + \frac{1}{L_m} u \quad (16) \quad e = x_{5ref} - x_5 \quad (17)$$

$$s = e \quad (18)$$

The STSMC algorithm is a second-order SMC technique that ensures finite-time convergence of the sliding variable and its derivative without requiring the measurement of higher-order derivatives. Compared with conventional first-order SMC, STSMC significantly reduces chattering while preserving robustness against matched uncertainties. The application of STSMC relies on the assumption that the system has a relative degree of

$$\begin{cases} u_{st} = -k_1 |s|^{\frac{1}{2}} \text{sgn}(s) + z \\ \dot{z} = -k_2 \text{sgn}(s) \end{cases} \quad (19)$$

The Lyapunov function proposed in (22) satisfies the positive-definiteness condition. Equation (23) is obtained by taking the derivative of $V(s,z)$ and combining it with (19) and (21). With k_1 and k_2 chosen as positive coefficients, the derivative of the proposed Lyapunov function becomes negative definite. Therefore, the system is considered stable.

$$V(s, z) = k_1 |s| + \frac{1}{2} z^2 \quad (22) \quad \dot{V}(s, z) = k_2 \text{sgn}(s) \dot{s} + z \dot{z} = -k_1 k_2 |s|^{\frac{1}{2}} \quad (23)$$

The control law described above does not account for the influence of parameter uncertainties. To enhance the robustness of the system against such uncertainties, the control parameter (k_1) is adjusted through a fuzzy algorithm, as described in (24). The output of the fuzzy logic system (k_s) is determined

one with respect to the sliding surface and that the lumped disturbances, including parameter uncertainties, are bounded and Lipschitz continuous. Under these conditions, the appropriate selection of control gains ensures the closed-loop system's finite-time stability. In the considered EPS system, these assumptions are satisfied, which justifies the use of the STSMC-based control law in this work.

$$u = L_m u_{st} + K_t x_4 + R_m x_5 + L_m \dot{x}_{5ref} \quad (20)$$

$$\dot{s} = \dot{x}_{5ref} + \frac{K_t}{L_m} x_4 + \frac{R_m}{L_m} x_5 - \frac{1}{L_m} u(t) = -u_{st} \quad (21)$$

according to (25). The firing strength (w_i) is computed using (26), where μ denotes the membership degree. Equation (27) provides the formulation for determining the corresponding rule output, where a_i and b_i are linear coefficients and c_i is a constant coefficient.

$$k_{1new} = k_1 k_s \quad (24)$$

$$k_s = \frac{\sum_{i=1}^n w_i f_i}{\sum_{i=1}^n w_i} \quad (25)$$

$$w_i = \mu_{|s|}^{(i)}(|s|) \mu_{|\dot{s}|}^{(i)}(|\dot{s}|) \quad (26)$$

$$f_i = a_i |s| + b_i |\dot{s}| + c_i \quad (27)$$

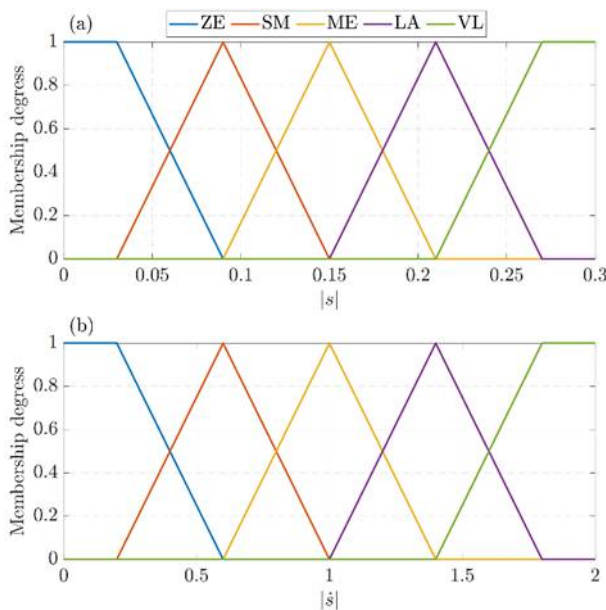


Figure 2. Membership function.
(a) The first input (b) The second input

The first and second inputs of the fuzzy system are absolute values of the sliding surface and its derivative, respectively. In the proposed fuzzy logic scheme, the sliding surface derivative is introduced to capture the

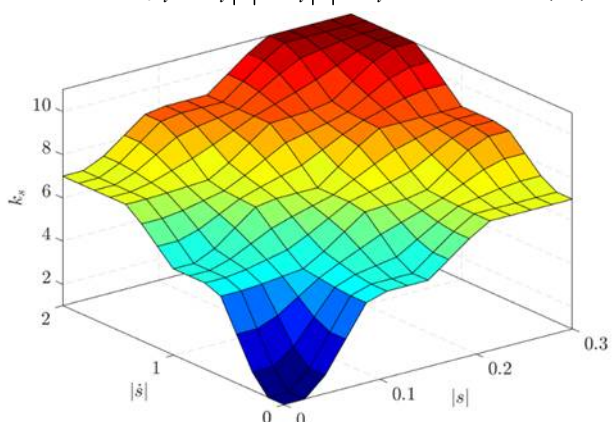


Figure 3. Fuzzy surface.

dynamic evolution of the tracking error. While the sliding surface reflects the instantaneous magnitude of the tracking error, its derivative provides information about its convergence trend and rate. By incorporating

the sliding surface derivative as an additional input, the fuzzy system can distinguish between approaching and diverging trajectories, allowing for adaptive adjustment of the control gain to accelerate convergence when necessary and to minimize excessive control action near the sliding surface. This mechanism improves transient performance and contributes to chattering suppression in the STSMC framework. The structure of membership functions is illustrated in Figure 2. The relationship between the output and inputs is represented by the fuzzy surface shown in Figure 3. Compared to conventional SMC or STSMC schemes that employ fixed control gains, the incorporation of fuzzy logic provides additional flexibility in handling systems. Traditional controllers rely on constant gain selection, which often involves a trade-off between fast convergence and chattering suppression. By contrast, the fuzzy logic mechanism dynamically adjusts the control gain according to the sliding surface and its derivative, enabling more decisive control action during large deviations and smoother behavior near the sliding surface. As a result, the proposed fuzzy-enhanced STSMC improves transient performance and robustness while further reducing chattering without increasing controller complexity.

The vehicle dynamic model is incorporated to characterize the variation of road reaction torque acting

on the EPS system. This interaction affects the steering dynamics and appears in the control-oriented model as a lumped disturbance term. Instead of being directly controlled, the vehicle dynamics influence the controller design through their impact on the evolution of the sliding surface. Consequently, the proposed STSMC-based control law is designed to robustly compensate for these effects without requiring explicit control of the vehicle dynamics.

3. Simulation results

The numerical simulations are carried out in MATLAB/Simulink to validate the performance of the proposed control scheme. The steering torque input is modeled as a periodic sinusoidal function, expressed as $T_d = 8\sin(2t)$. The steering maneuver is examined at a medium vehicle speed of $v = 40\text{km/h}$, which reflects typical urban driving conditions. Two cases are considered in this study. In the first case, parameter uncertainties are not included. In contrast, in the second case, uncertainties in the torque coefficient (ΔK_t) and motor resistance (ΔR_m) are introduced, with increases of 15% and 10%, respectively. The objective is to examine the robustness of proposed control relative to conventional SMC, given that their control laws do not explicitly address the influence of parameter uncertainties. The specifications of the system are listed in Table 1.

Table 1. Specifications

Symbol	Unit	Value	Symbol	Unit	Value	Symbol	Unit	Value
K_c	Nm/rad	135	l_n	m	0.3	γ_k	°	10
B_c	Nms/rad	0.066	J_ψ	kgm ²	3080	γ_c	°	3
J_c	kgm ²	0.064	m_r	kg	27	m	kg	1400
N	-	20	R_m	Ω	0.46	L_m	H	0.004
r_p	m	0.015	B_m	Nms/rad	0.0045	l_1	m	1.22
K_t	Nm/A	0.05	B_r	Ns/m	3350	l_2	m	1.64
l_c	m	0.03	J_m	kgm ²	0.0005	K_α	N/m	45500

The simulation outputs include the steering column angle (SCA), steering column speed (SCS), steering motor angle (SMA), steering motor speed (SMS), motor current, and the assisted torque.

3.1. The first case without parameter uncertainties

The variations in the system's dynamic behaviors under sinusoidal steering at a medium speed ($v = 40\text{ km/h}$) are illustrated in the subplots of Figure 4. A closer examination of Figure 4a reveals that the SCA signals generated by both controllers closely follow the reference input. According to the analysis, the RMS tracking error of the proposed controller is only about 0.019%, which is significantly lower than that of the conventional SMC (0.178%). The window plot in Figure 4b shows that the FSTSMC achieves slightly better tracking performance compared with the conventional SMC, reducing the RMS tracking error to

0.014% compared with 0.162% for SMC. Similarly, the SMA and SMS responses obtained from the proposed controller exhibit lower tracking errors than those produced by SMC, although the differences are relatively small.

The results in Figure 5a show that the motor current obtained from both controllers tends to follow the reference signal. However, noticeable chattering appears in the conventional SMC, causing the RMS tracking error to increase to 0.035 A, equivalent to 0.514%. By leveraging the STSMC technique, this phenomenon is significantly mitigated, resulting in a reduction of the RMS tracking error to only 0.037%. The relationship between the assisted torque and the driver torque is illustrated in Figure 5b. Overall, the proposed FSTSMC scheme offers superior control performance compared to the conventional SMC, effectively reducing both chattering and errors.

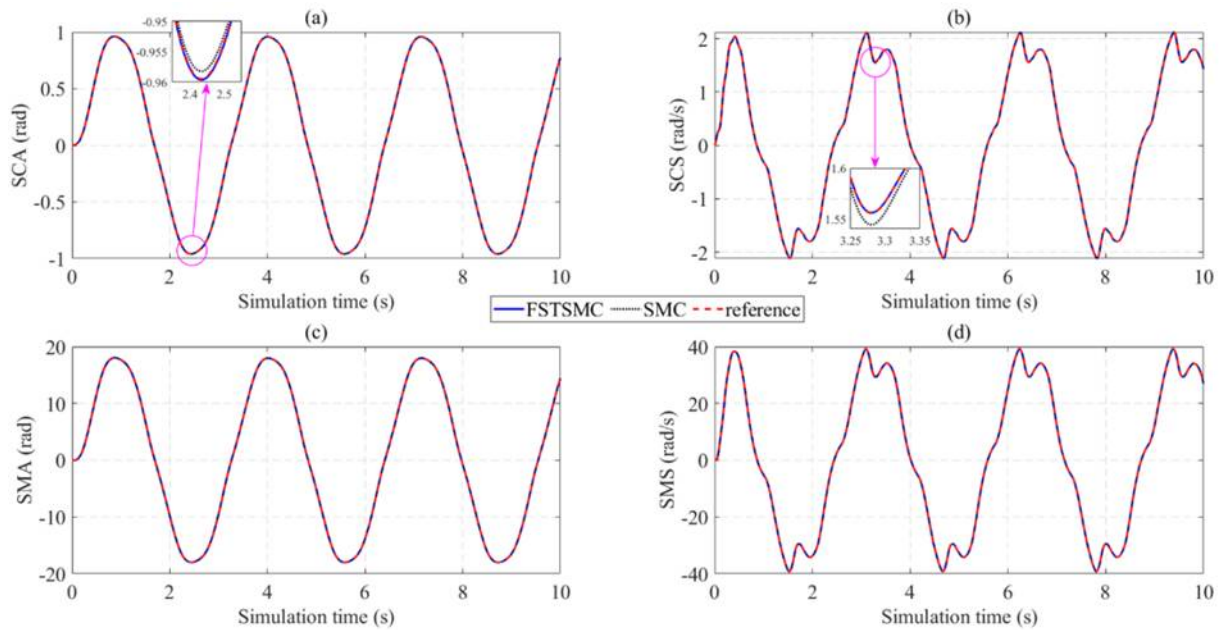


Figure 4. Actuator dynamics (1st case).

- (a) Steering column angle (b) Steering column speed
(c) Steering motor angle (d) Steering motor speed

3.2. The second case with parameter uncertainties

In the second case, the parameter uncertainties are increased to approximately 15% (Figure 6). The simulation results in Figure 6a indicate that the tracking error increases as the level of uncertainty rises. When uncertainties are not accounted for in the control law, the conventional SMC fails to maintain system robustness, resulting in a tracking error that increases to 31.028%. Under the effective control of the STSMC, with control parameters tuned through the fuzzy logic scheme, the tracking error is significantly reduced to 3.039%.

Figure 6b further demonstrates that the RMS tracking error obtained from the proposed FSTSMC is only 3.367%, which is substantially lower than that of the conventional SMC (36.569%) when uncertainties are included in the simulation. Overall, the tracking error of the conventional SMC is more than an order of magnitude higher than that of the proposed controller, as illustrated in Figures 6c and 6d.

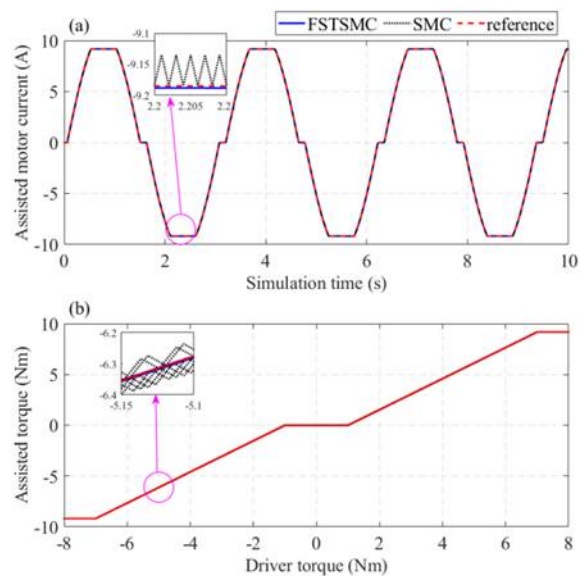
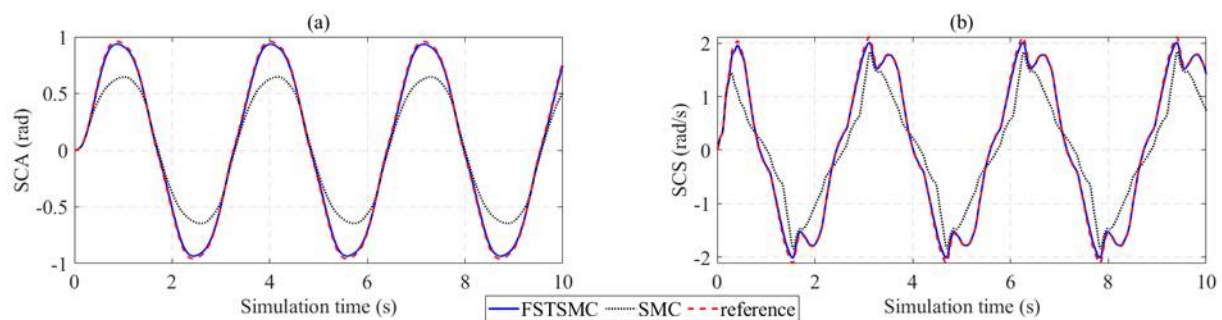


Figure 5. Actuator performance (1st case).

- (a) Steering motor current (b) Assisted torque



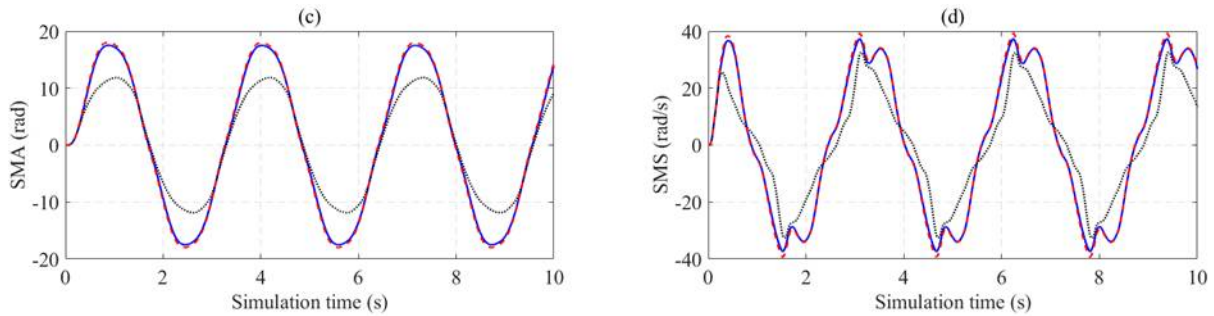


Figure 6. Actuator dynamics (2nd case).

- (a) Steering column angle (b) Steering column speed
(c) Steering motor angle (d) Steering motor speed

Figure 7a illustrates the degradation in SMC performance when the system is subjected to parameter uncertainties, causing the tracking error to rise to 5.867 A (60.195%). When the proposed controller replaces the conventional SMC, the RMS tracking error is significantly reduced to 3.559%. Additionally, the chattering phenomenon is significantly suppressed. As shown in Figure 7b, the assisted torque generated by the FSTSMC closely follows the ideal reference, whereas the conventional SMC exhibits a considerable deviation, leading to reduced control performance.

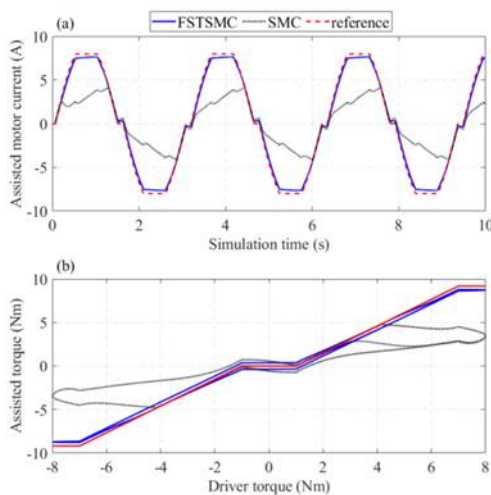


Figure 7. Actuator performance (2nd case).

- (a) Steering motor current (b) Assisted torque

4. Conclusion

This study presents the design of a robust control mechanism that combines the Super-Twisting Sliding Mode Control with a fuzzy logic scheme. This integration proves highly effective in reducing tracking errors and eliminating chattering, even when the system is subjected to parameter uncertainties. The system performance can be further improved by incorporating an active disturbance rejection mechanism into the proposed control framework. This represents a promising direction for future research with strong potential for practical implementation.

Funding

This research is funded by Thuyloi University Foundation for Science and Technology under grant number TLU.STF.25-04.

References

- D. Lee, et al. (2019). *A development of the model based torque feedback control with disturbance observer for electric power steering system*, SAE Technical Papers.
- M. B. Baharom, K. Hussain, A. J. Day (2013). *Design of full electric power steering with enhanced performance over that of hydraulic power-assisted steering*, Proceedings of the Institution of Mechanical Engineers, Part D: Journal of Automobile Engineering, vol. 227, no. 3, pp. 390–399.
- M. Irmer and H. Henrichfreise. (2020). *Design of a robust LQG compensator for an electric power steering*, IFAC PapersOnLine, vol. 53, no. 2, pp. 6624–6630.
- M. K. Hassan, et al. (2012). *Optimal design of electric power assisted steering system (EPAS) using GA-PID method*, Procedia Engineering, vol. 41, pp. 614–621.
- S. Kim, M. Choi, and J. Sung (2023). *Experimental verifications of electric power steering controller based on discrete-time sliding mode control with disturbance observer*, International Journal of Automotive Technology, vol. 24, no. 3, pp. 883–888.
- T. A. Nguyen (2025). *A linear quadratic tracking control strategy based on fuzzy for electric power steering systems*, Advances in Mechanical Engineering, vol. 17, no. 2.
- W. Zhao and H. Zhang (2018). *Coupling control strategy of force and displacement for electric differential power steering system of electric vehicle with motorized wheels*, IEEE Transactions on Vehicular Technology, vol. 67, no. 9, pp. 8118–8128.
- Y. Li, et al. (2019). *Dual-motor full-weight electric power steering system for commercial vehicle*, International Journal of Automotive Technology, vol. 20, no. 3, pp. 477–486.
- Z. A. Zheng and J. C. Wei (2023). *Research on electric power steering fuzzy PI control strategy based on phase compensation*, International Journal of Dynamics and Control, vol. 11, pp. 1867–1879.